Vietnam Journal of Earth Sciences, 44(2), 181-194, https://doi.org/10.15625/2615-9783/16764

Vietnam Academy of Science and Technology
Vietnam Journal of Earth Sciences
http://www.vjs.ac.vn/index.php/jse

Pore water pressure responses of saturated sand and clay under undrained cyclic shearing

Tran Thi Phuong An[1], Hiroshi Matsuda[2], Tran Thanh Nhan[1*], Nguyen Thi Thanh Nhan[1], Pham Van Tien[3], Do Quang Thien[1]

[1]*University of Sciences, Hue University, 77 Nguyen Hue, Hue, Vietnam*
[2]*Yamaguchi University, 2-16-1 Tokiwadai, Ube, Yamaguchi, 755-8611, Japan*
[3]*Institute of Geological Sciences, VAST, Hanoi, Vietnam*

Received 02 September 2021; Received in revised form 20 October 2021; Accepted 01 December 2021

ABSTRACT

In this study, changes in the pore water pressure were observed for saturated specimens of a loose fined-grain sand (Nam O sand) and a soft silty clay (Hue clay) subjected to undrained cyclic shearing with different testing conditions. The cyclic shear tests were run for relatively wide range of shear strain amplitude (γ = 0.05%-2%), different cycle numbers (n = 10, 50, 150 and 200) and various shear directions (uni-direction and two-direction with phase difference of θ = 0°, 45° and 90°). It is indicated from the experimental results that under the same cyclic shearing condition, the pore water pressure accumulation in Hue clay is at a slower rate, suggesting a higher cyclic shear resistance of Hue clay than that of Nam O sand. Liquefaction is reached easily in nominally 50% relative density specimens of Nam O sand when $\gamma \geq$ 0.4%, meanwhile soft specimen of Hue clay is not liquefied regardless of the cyclic shearing conditions used in this study. The threshold number of cycles for the pore water pressure generation generally decreases with γ meanwhile, the threshold cumulative shear strain for such a property mostly approaches 0.1%. In addition, by using this new strain path parameter, it becomes more advantageous when evaluating the pore water pressure accumulation in Nam O sand and Hue clay subjected to undrained uni-directional and two-directional cyclic shears.

Keywords: Cyclic shear, effective stress, Nam O sand, pore water pressure, Hue clay.

1. Introduction

When a saturated layer of soil deposits is subjected to cyclic loading (earthquakes, traffic loads, pile driving, ocean waves, or explosions), pore water pressure is increased. Under undrained conditions characterized by low permeability of the soil layer, limited pore water pressure dissipation, and short durations of loading application, cyclic shear-induced

*Corresponding author, Email: ttnhan@hueuni.edu.vn

pore water pressure is accumulated. For sandy soils at loose density, the pore water pressure increases rapidly and quickly, equal to the initial vertical stress of the liquefaction condition (Seed 1979). As the time proceeds after the cyclic loading event, the cyclic-induced pore water pressure dissipates and results in the recompression of the soils which occurs at the ground surface as vertical settlement. The so-called liquefaction-induced settlements have been observed in significant earthquakes such as the 1964 Niigata earthquake. Significant liquefaction-induced settlements led to the massive damage of buildings all over Niigata City (Tokue 1976). After the 2011 Tohoku Pacific earthquake, the liquefaction occurred in the extensive of reclaimed areas constituting of sand, sandy soils, and other materials (Tokimatsu and Katsumata, 2012; Bhattacharya et al., 2011), accompanied by excessive ground settlement up to 60 cm as well as the settlement and tilting of structures supported on spread foundation.

Compared with the cyclic shear resistance of sand, cohesive soils with cohesion are believed to be relatively stable and hardly liquefied even under a strong motion from the earthquakes (Yasuhara et al., 1992; 2001). The cyclic shear-induced pore water pressure in clay layers, however, may develop to a relatively high level (Ohara et al., 1981), resulting in cyclic failure, which has been widely confirmed (Yasuhara and Andersen 1991; Gratchev et al., 2006; Sasaki et al., 1980; Mendoza and Auvinet 1988). Soft ground may gradually settle due to the dissipation of cyclically induced pore pressures which has been typically observed after significant earthquakes such as the Mexico earthquake in 1957 (Zeevaert 1983), the Miyagi-ken Oki earthquake in 1978 (Suzuki 1984), and the Hyogo-ken Nanbu earthquake in 1995 (Matsuda 1997).

Soft soils of Phu Bai formation ($ambQ_2^{1-2}$ *pb*) and fine- to medium-grained sands of Nam O formation (mvQ_2^2 *no*) continuously spread in Thua Thien Hue and Quang Tri provinces. In Thua Thien Hue province, the clayey soils of Phu Bai formation stratify close to the ground surface in Hue city and surrounding areas, while the sandy soils of Nam O formation are mainly exposed to ground surface along the coastal plains (Fig. 1). Consequently, such soils significantly affect the stability of structures and economic efficiencies of the construction in the area. According to Vietnamese Standard TCVN 9386:2012 (MOST 2012), the ground acceleration is from a = 0,0275g to a = 0,0612g in Quang Tri and from a = 0,0434g to a = 0,0804g in Thua Thien Hue and therefore, potential earthquake intensity in this region is between V and VII (MSK-64 scale). Consequently, the dynamic behaviors of the ground, especially the cyclic shear resistance and the liquefaction potential of weak soils, should be considered in the design specification of structures. In this study, a silty clay that partly constitutes Phu Bai formation and the fine-grained sand of Nam O formation was used for the cyclic shear test. Based on this, pore water pressure responses of the soils were then clarified under the effects of different cyclic shearing conditions.

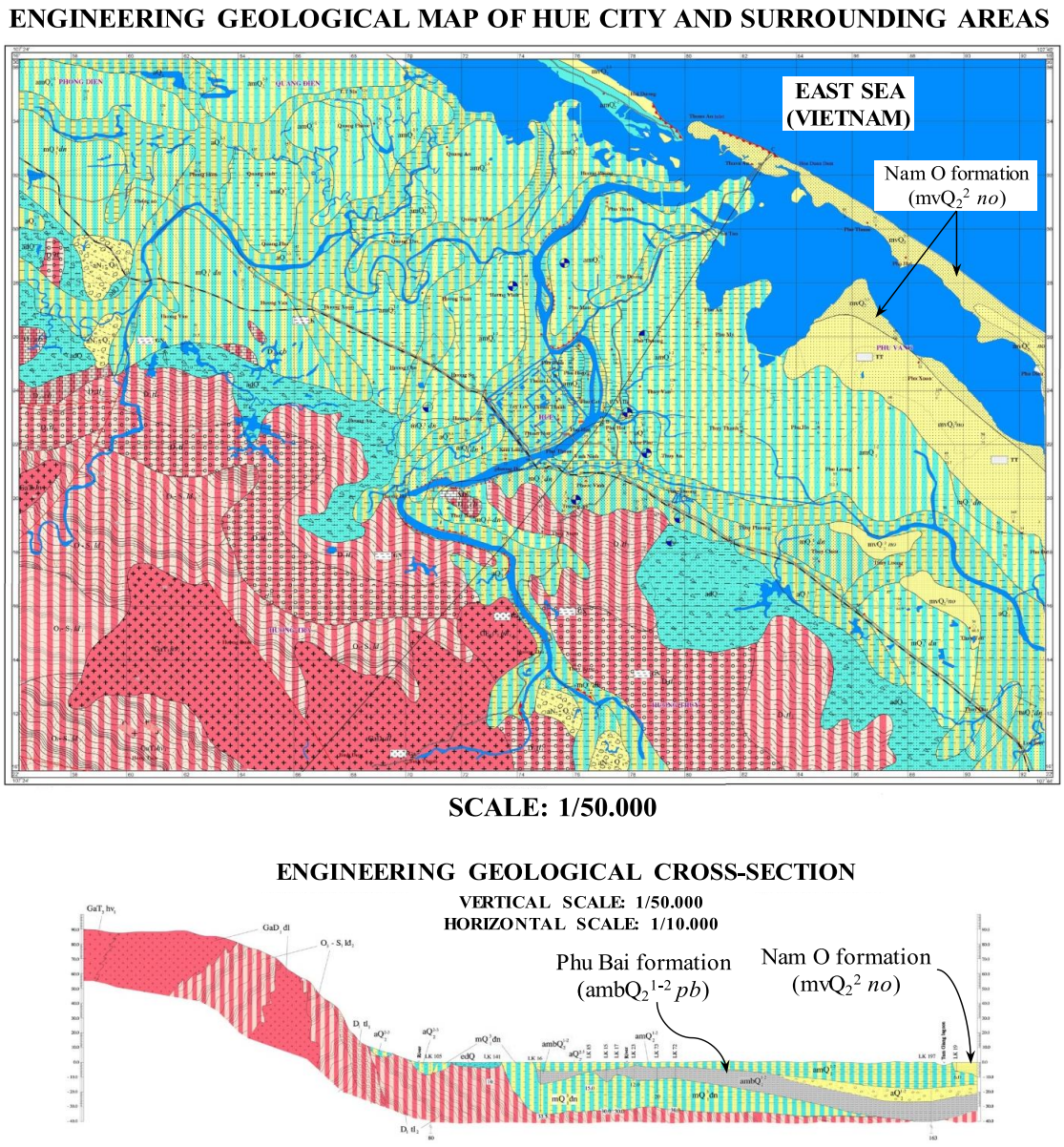

Figure 1. Engineering geological map and cross-section for Hue city and surround areas (Vy 2007)

2. Details of cyclic shear test series

2.1. Material, apparatus and preparation

As mentioned above, a silty clay partly constitutes Phu Bai formation, and fine-grained sand of Nam O formation (from now on referred to as Hue clay and Nam O sand, respectively (Nhan 2019, Nhan and Matsuda 2020)) were used for this study. The grain size distribution curves of the soils are shown in Fig. 2, and physicomechanical properties are summarized in Table 1.

In order to prepare specimens of Hue clay, reconstituted samples of the soil were mixed with de-aired water to reach a slurry state at a water content of about 1.5 times its liquid

limit (i.e. $w = 1.5 \times w_L = 41.1\%$) and kept under constant water content for one day. Based on the standard penetration test data obtained for sandy soils constituting of Nam O formation in the study area, the relative density of Dr = 41%-58.3% was confirmed for the distribution depth $H \leq 19.5$ m (from the ground surface (Tin 2019)) and therefore, the target relative density of soil specimen used in this study was fixed as D_r = 50% and correspondingly, soil specimen has a dry density of ρ_d = 1.461 g/cm^3 and void ratio e = 0.807. The dried soil samples at predetermined volumes intended to produce Dr = 50% were then mixed with de-aired water so that the sand was immersed in water and kept for one day in a plastic box with a lid. The slurry of Hue clay and sand-mixed water of Nam O sand was then de-aired in the vacuum cell before pouring into a rubber membrane in the Kjellman shear box of the multi-directional cyclic simple shear test apparatus developed at Yamaguchi University, Japan (Fig. 3a).

By using a stack of acrylic rings, lateral expansion of the membrane-enclosed specimen is prevented and therefore, the specimen is cyclically sheared under a constant cross-sectional area. Photo of the test apparatus including situation of the specimens of Nam O sand and Hue clay in the shear box are shown in Fig. 3.

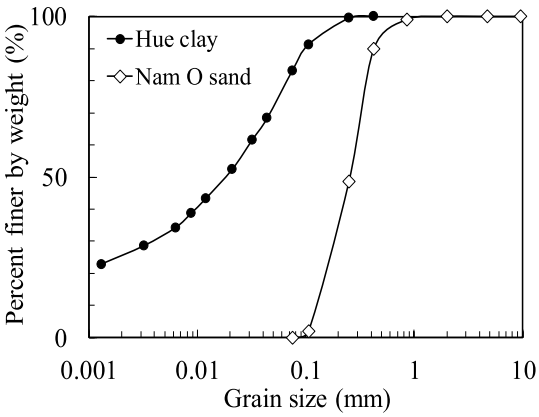

Figure 2. Grain size distribution curves of tested soils

Table 1. Physico-mechanical properties of tested soils

Soil / Property	Nam O sand	Soil / Property	Hue clay
Specific gravity, G_s	2.64	Specific gravity, G_s	2.68
Maximum void ratio, e_{max}	0.960	Liquid limit, w_L (%)	29.4
Minimum void ratio, e_{min}	0.653	Plastic limit, w_P (%)	18.7
Coefficient of uniformity, U_c	2.30	Plasticity index, I_p	10.7
Coefficient of curvature, U'_c	0.91	Compression index, C_c	0.20
Effective diameter, D_{10} (mm)	0.126	Swelling index, C_s	0.04

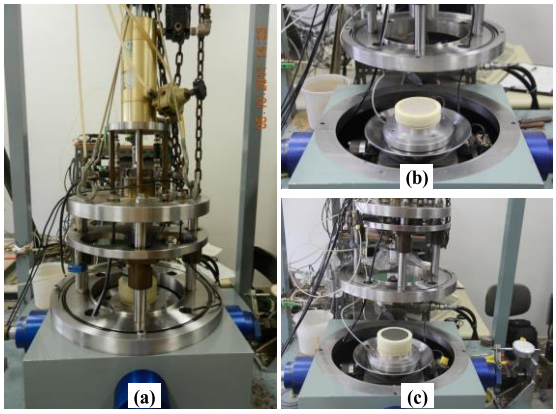

Figure 3. (a) Photo of the multi-directional cyclic simple shear test apparatus and situation of specimen of (b) Nam O sand and (c) Hue clay in the shear box

2.2. Test procedures and conditions

The slurry was then consolidated under the vertical stress of σ_{vo} = 49 kPa until the dissipation of pore water pressure at the bottom surface of the specimen was confirmed. After the consolidation, soil specimens have the dimensions of 75 mm in diameter and 20 mm in height, and with an average void ratio of e = 0.731 for Hue clay and relative density of D_r = 50%±5% for Nam O sand were subjected to undrained uni-directional and two-directional cyclic shears.

In order to meet the effect of loading

frequency in nature especially those during major earthquakes, cyclic shear tests for investigating the dynamic behavior of soil deposits often apply the frequency $f \geq 0.1$ Hz (Talesnick and Frydman 1992) and therefore, the cyclic shear test in this study was run with $f = 0.5$ Hz ($T = 2.0$ s). The shear strain amplitude, defined by the ratio of maximum horizontal displacement to the initial specimen height, was in the range from $\gamma = 0.05\%$ to 2.0%. The number of cycles was changed from $n = 10$ to $n = 200$ (Table 2). Such conditions cover the loading amplitude and duration of major earthquakes. For the uni-directional cyclic shear test, the shear strain was applied to the specimen in one direction only (either in X direction or Y direction); meanwhile, for the two-directional ones, cyclic shear strains were simultaneously applied in both X and Y directions at the same amplitude (i.e. $\gamma = \gamma_X = \gamma_Y$) but with the degree of phase shift fixed as $\theta = 0^o$, 45^o and 90^o. The conditions of the cyclic shear tests are shown in detail in Table 2.

Table 2. Conditions for undrained cyclic shear tests

Soil	f (Hz)	n	Uni-direction	Two-direction	
			γ (%)	θ (^{o})	γ (%)
Hue clay	0.5	200	0.05, 0.1, 0.2, 0.4, 1.0	45^o, 90^o	0.1, 0.2, 0.4, 1.0
Nam O sand	0.5	10, 50, 150	0.1, 0.2, 0.4, 1.0, 2.0	0^o, 45^o, 90^o	0.1, 0.2, 0.4, 1.0

2.3. A strain path parameter for the cyclic simple shear strains

Under the undrained cyclic shearing, the pore water pressure is generated and accumulated by applying the cyclic shear strain. The longer the strain path of soil particle movement, the more the structure disturbance and the cyclic degradation that the soil would experience. Matasovic and Vucetic (1992, 1995) indicated that the cyclic resistance of soil is significantly affected by the pore water pressure accumulation. The level of cyclic shear-induced pore water pressure accumulation is related to the cyclic degradation of cohesive soils. Such observations mean that the length of the cyclic shear strain path can be used when evaluating soil's cyclically induced pore water pressure responses. Fukutake and Matsuoka (1989) proposed a so-called Bowl model to describe the movement of soil particles during cyclic shearing by using a new strain path parameter, which is named as cumulative shear strain (G*) and defined by Eq. (1) as follows:

$$G^* = \Sigma \Delta G^* = \Sigma (\Delta\gamma_x^2 + \Delta\gamma_y^2)^{0.5} \quad (1)$$

where $\Delta\gamma_x$ and $\Delta\gamma_y$ are the shear strain increment in two orthogonal directions, *i.e.,* X and Y directions, respectively.

Eq. (1) indicates that G^* denotes the summation of the increment of shear strain on the horizontal plane during cyclic shear and therefore, G^* increases with the amplitude (i.e. γ) and the application duration (i.e., n) of the cyclic shear. Consequently, by applying Eq. (1) to recorded data of the cyclic shear test, relations of G^* versus n and γ were proposed for the uni-directional and two-directional cyclic shears as Eqs. (2) and (3), respectively (Matsuda et al., 2013; Nhan, 2013).

Uni-direction: $G^* = n\ (3.950\ \gamma + 0.0523)$ (2)

Two-direction: $G^* = n\ (5.995\ \gamma + 0.3510)$ (3)

At staring point of the cyclic shearing, G^* should be zero meaning that Eqs. (2) and (3) should be modified. Recently, the $G^* - \gamma - n$ relation has been firstly improved for the case of gyratory cyclic shear strain (i.e. $\theta = 90^o$) as Eq. (4) as follows (Nhan and Matsuda, 2020):

$$G^* = 6.2825 \times \gamma \times n \quad (4)$$

In Fig. 4, the cumulative shear strain G^* is shown for various cyclic shear directions, a

wide range of γ = 0-2.0% and different number of cycles n = 10-200 (Nhan 2013, Nhan et al., 2022). Symbols in the figures show the observed results of G^* by applying Eq. (1) to recorded data of the cyclic shear test, meanwhile dashed- and solid-lines correspond to the correlations of G^* versus γ and n following Eqs. (5) and (6) for the uni-directional and two-directional cyclic shears, respectively.

Uni-direction: $G^* = 4 \times \gamma \times n$ (5)

Two-direction: $G^* = 6.3084 \times \gamma \times n$ (6)

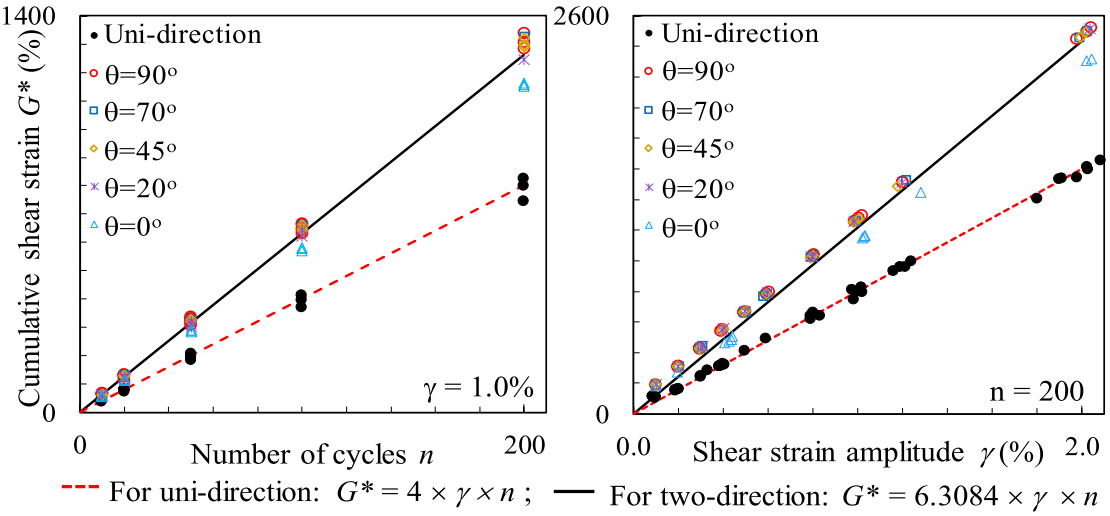

Figure 4. Relations of G^* versus γ and n for various cyclic shear directions (Nhan 2013; Nhan et al., 2022)

3. Results and discussions

3.1. Changes of effective stress and pore water pressure during undrained cyclic shears

Under the cyclic shearing, the vertical stress of saturated specimen of Nam O sand was automatically adjusted so that the height of specimen was kept unchanged and based on which, the undrained (constant-volume) condition was simulated. In addition, the decrement in the effective stress ($|\Delta\sigma'_v|$) under constant-volumed condition is assumed to be equal to the increment in the pore water pressure (i.e. $|\Delta\sigma'_v| = u_{acc}$) under fully saturated condition (in order to satisfy the saturation of specimen, B-value defined by the ratio of the pore water pressure increment to the vertical stress increment was confirmed to be over 0.95 before the undrained cyclic shear) which was applied for Hue clay. In this study, the terms of pore water pressure accumulation was used for such undrained conditions. In Fig. 5, typical changes of the pore water pressure ratio, defined by u_{acc}/σ'_{vo} where σ'_{vo} is the initial effective stress, are shown for Nam O sand and Hue clay subjected to different cyclic shear conditions.

It is seen that u_{acc}/σ'_{vo} increases with the logarithm of n and at the same n, cyclic shear with larger amplitude (γ) results in higher u_{acc}/σ'_{vo}. When comparing the test results between the soils, the accumulation of pore water pressure on Hue clay is at a slower rate resulting in lower values of u_{acc}/σ'_{vo} than that on Nam O sand under similar cyclic shearing conditions. Also in Fig. 5, nominally 50% relative density specimen of Nam O sand shows a sudden increase in u_{acc}/σ'_{vo} and liquefaction is reached after several cycles when $\gamma \geq 0.4\%$. At smaller shear strain amplitudes (i.e. γ = 0.1% and 0.2%), u_{acc}/σ'_{vo} gradually increases and the larger number of cycles are required for liquefaction. In contrast,

liquefaction is not reached in Hue clay regardless the cyclic shearing conditions used in this study (i.e. n = 200, γ = 0.1-1.0% and various cyclic shear directions). Cohesive soils with cohesion have been confirmed to be more stable and show higher cyclic shear resistance than granular soils when subjected to dynamic loading (Yasuhara et al., 1992; 2001). In this study, the liquefaction resistance of Hue clay with a relatively low plasticity (I_p = 10.7) is higher than that of Nam O sand at D_r = 50%±5%.

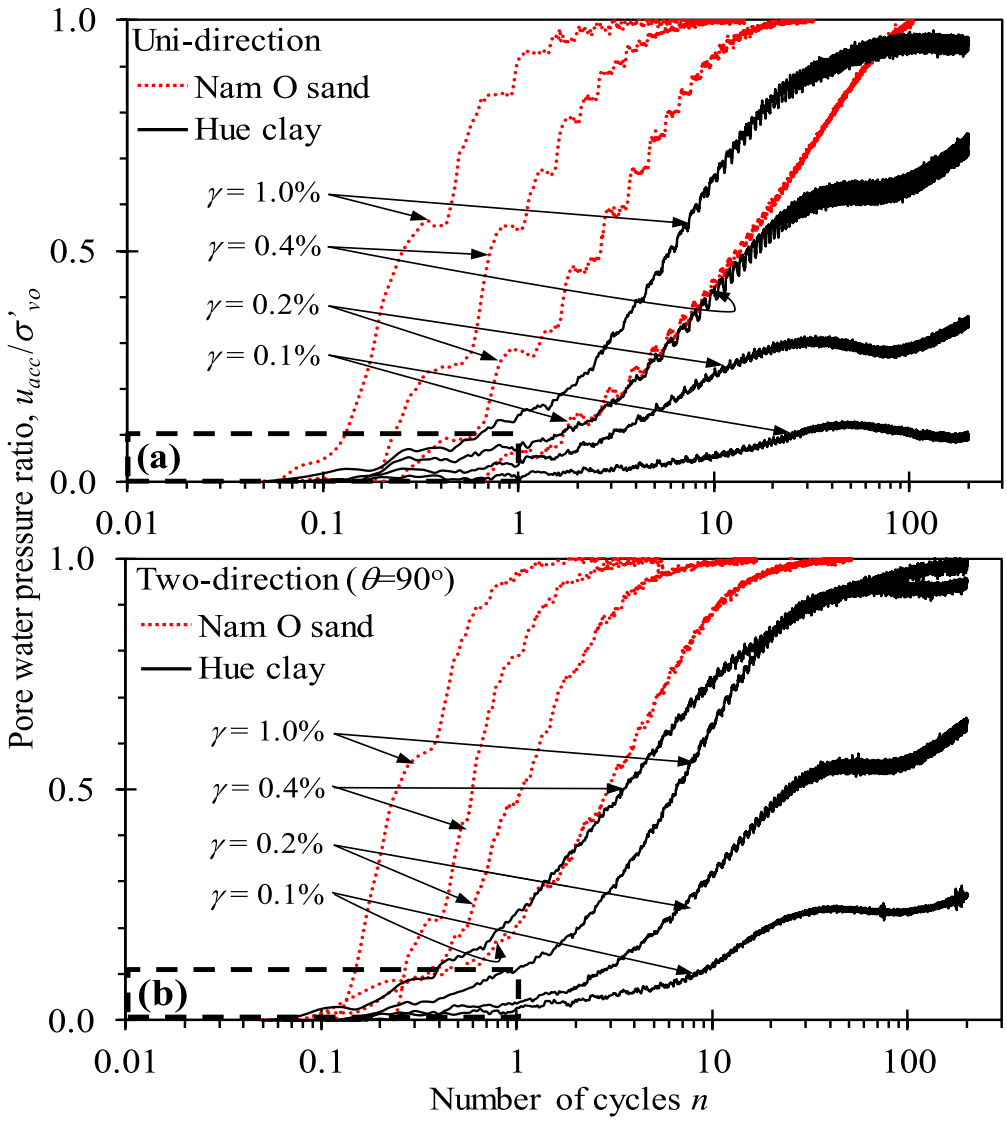

Figure 5. Changes of u_{acc}/σ'_{vo} in Nam O sand and Hue clay subjected to undrained cyclic shearing with different conditions

Observed results of u_{acc}/σ'_{vo} in Fig. 5 are plotted against G^* as shown in Fig. 6 to demonstrate the applicability of this parameter for describing the changes in pore water pressure during undrained cyclic shear. As mentioned previously, the cyclic

shear at a larger amplitude and a longer duration results in a longer strain path of soil particle movement. For each case of cyclic shear direction in Fig. 6, the tests at larger n and γ reveal larger values of G^* and for each soil, the larger G^* results in the higher u_{acc}/σ'_{vo}. In addition to Fig. 6, by using G^* instead of n, the tendencies of u_{acc}/σ'_{vo} between different shear strain amplitudes become more unique and the advantages of using G^* for capturing the effect of cyclic shear direction on the cyclic shear-induced pore water pressure are confirmed in this study and also in previous ones (Nhan 2013; Nhan and Matsuda 2020; Nhan et al., 2022).

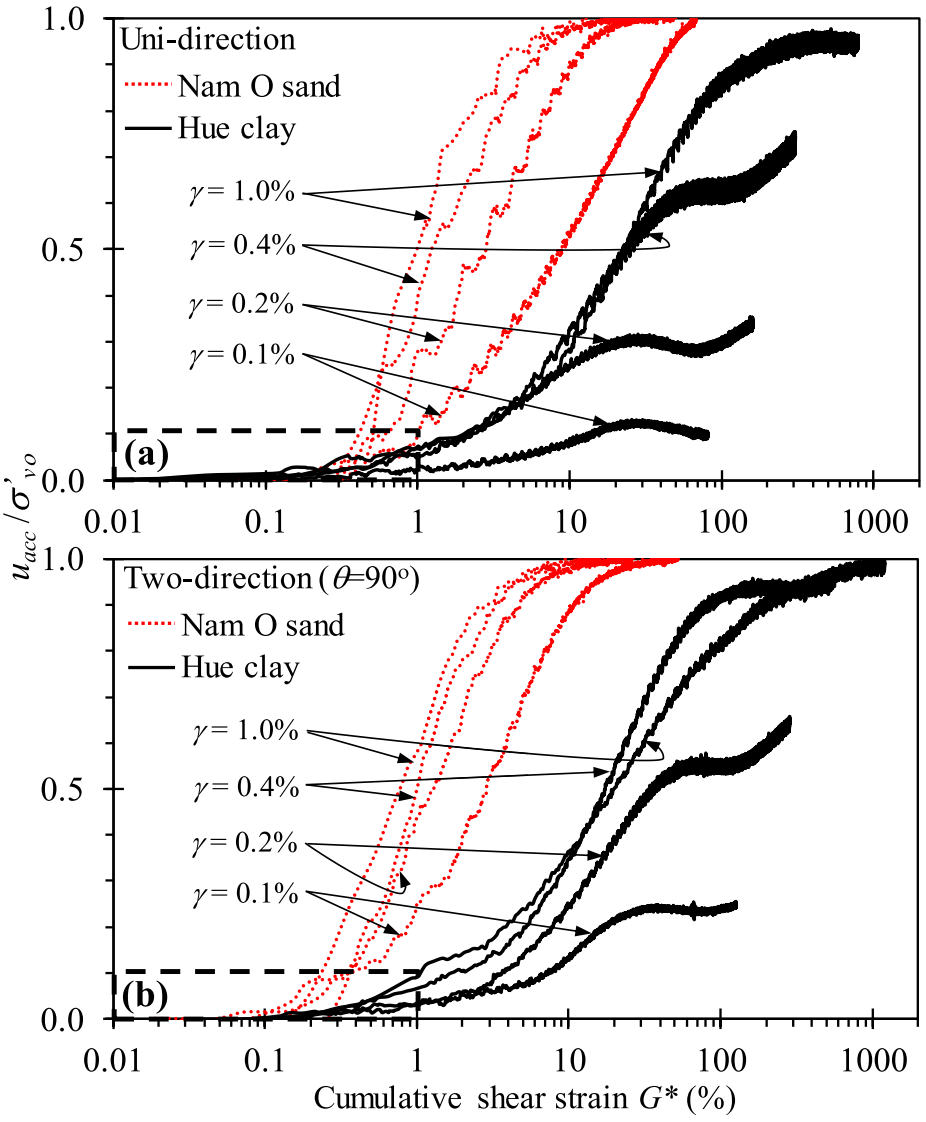

Figure 6. Relations between u_{acc}/σ'_{vo} and G^* on Nam O sand and Hue clay subjected to undrained cyclic shearing with different conditions

3.2. Threshold number of cycles and cumulative shear strain for the pore water pressure generation

In order to observe more in detail the pore water pressure generation, changes of u_{acc}/σ'_{vo} at early stage of the cyclic shearing in Figs. 5 and 6 (marked by dashed-retangular with vertical boundaries of u_{acc}/σ'_{vo} = 0.1 and horizontal boundaries of n = 1 and G^* = 1%) are shown in Figs. 7 and 8, respectively.

By using the plots in Figs. 7 and 8, the number of cycles and the cumulative shear strain at which the pore water pressures in Hue clay and Nam O sand start to generate can be measured for uni-directional and two-directional cyclic shears. These parameters are referred to as threshold number of cycles and threshold cumulative shear strain for pore water pressure generation in Nam O sand (symbolized by n_{tpNO} and G^*_{tpNO}, respectively) and Hue clay (symbolized by n_{tpHU} and G^*_{tpHU}, respectively). Obtained values of such parameters are summarized in Table 3 and their changes with γ are shown in Fig. 9.

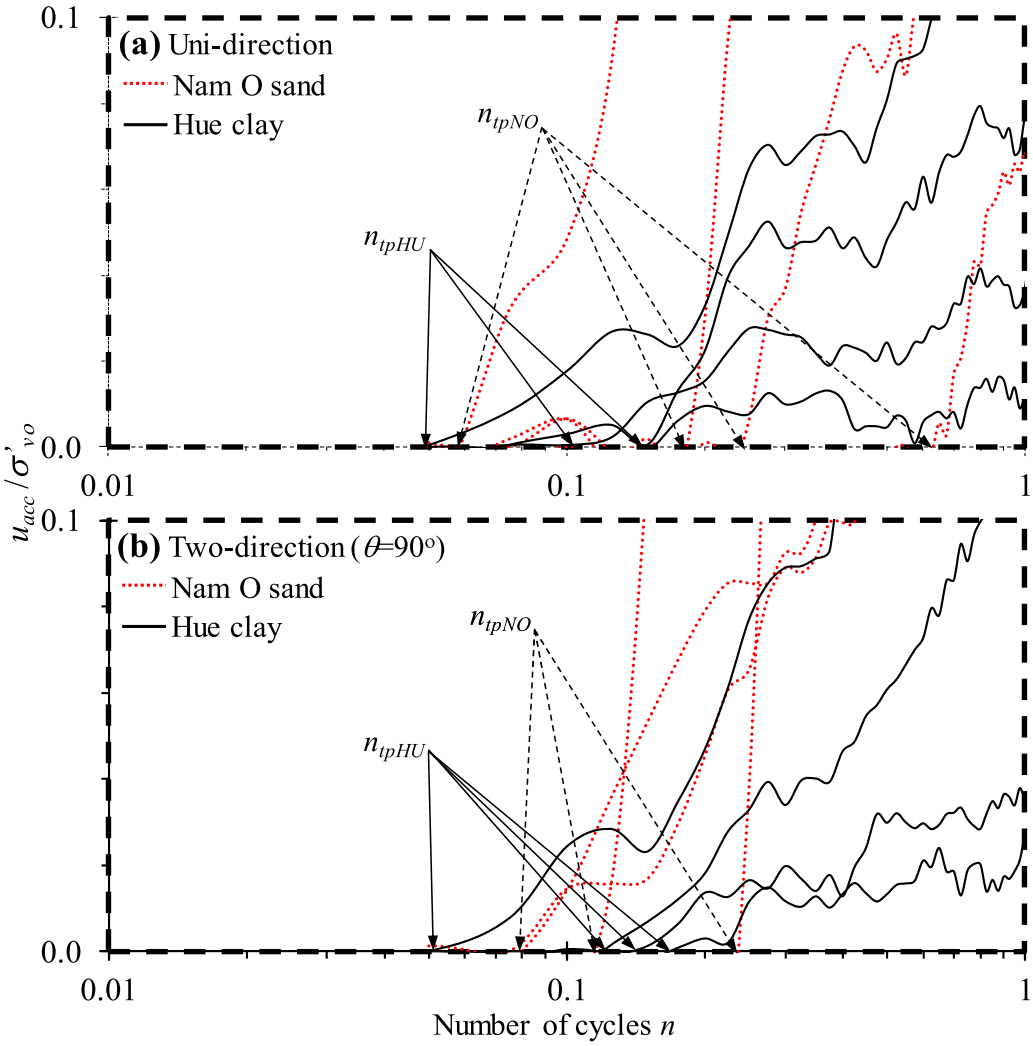

Figure 7. Changes of u_{acc}/σ'_{vo} with n at early stage of the undrained cyclic shear (Enlarge from the dashed retangular (a) and (b) in Fig. 5)

In Fig. 9(a), it is shown on each soil that values of n_{tpNO} and n_{tpHU} induced by the gyratory cyclic shear are slightly higher than those of the uni-directional one. When comparing the results between Nam O sand and Hue clay, n_{tpNO} is higher than n_{tpHU} regardless of the cyclic shear direction. Meanwhile, it is seen in Fig. 9(b) that changes of G^*_{tpNO} and G^*_{tpHU} with γ are in different situations and that, G^*_{tpNO} and G^*_{tpHU} mostly approach 0.1%. Consequently, G^*_{tpNO} = G^*_{tpHU} = 0.1% is considered as the threshold cumulative shear strain for the pore water pressure generation in Nam O sand and Hue clay subjected to undrained uni-directional and two-directional cyclic shears with the shear strain amplitude in the range from γ = 0.1% to 1.0%.

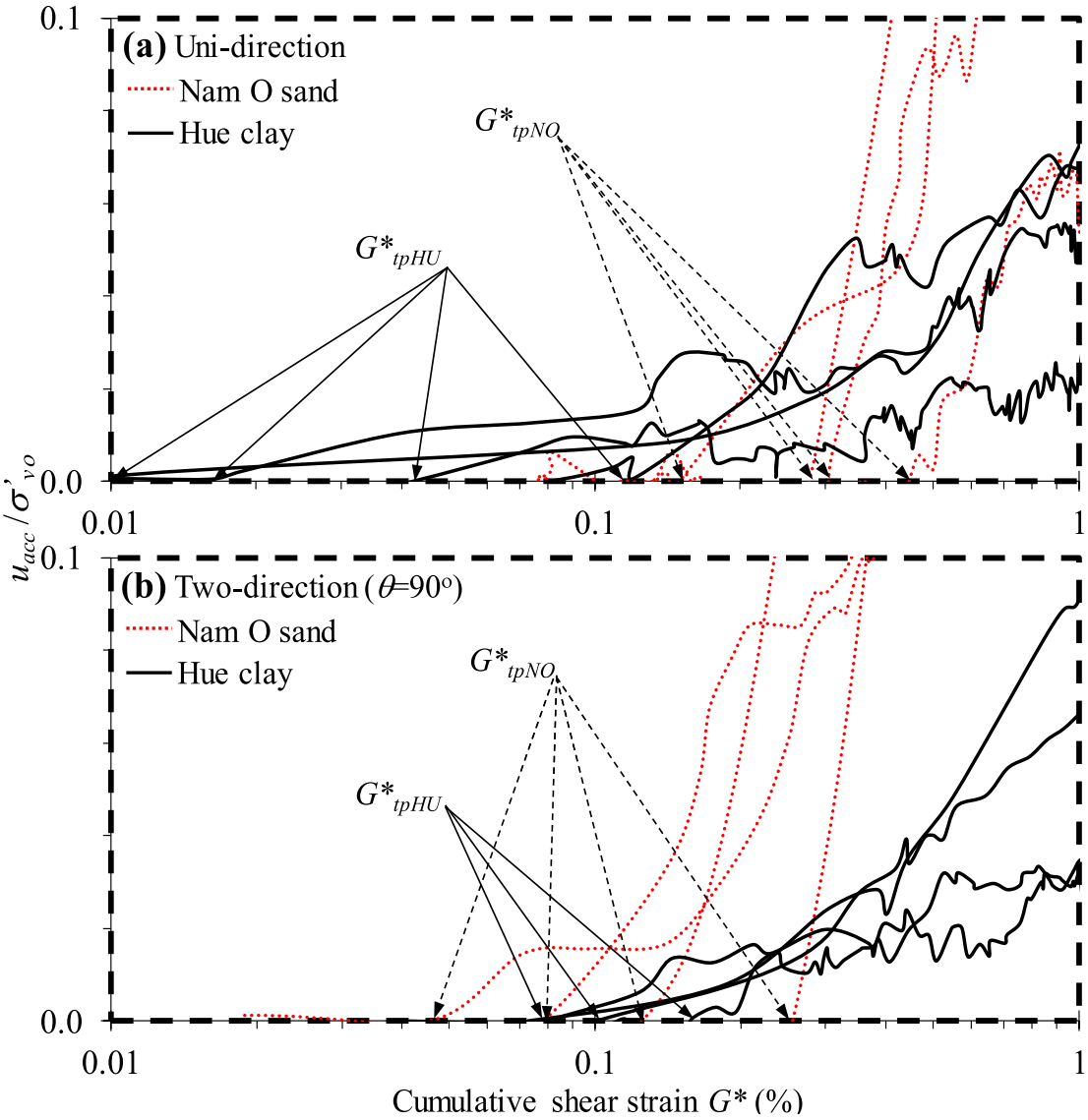

Figure 8. Changes of u_{acc}/σ'_{vo} with G^* at early stage of the undrained cyclic shear (Enlarge from the dashed retangular (a) and (b) in Fig. 6)

Table 3. Obtained values of n_{tpNO}, n_{tpHU}, G^*_{tpNO} and G^*_{tpHU} for uni-directional and gyratory cyclic shears

Soil	Shear direction	n_{tpNO} and n_{tpHU}				G^*_{tpNO} and G^*_{tpHU} (%)			
γ (%)		**0.1**	**0.2**	**0.4**	**1.0**	**0.1**	**0.2**	**0.4**	**1.0**
Nam O sand	Uni-direction	0.63	0.25	0.2	0.075	0.075	0.075	0.25	0.125
	$\theta = 90^o$	0.44	0.31	0.27	0.15	0.045	0.08	0.25	0.13
Hue clay	Uni-direction	0.15	0.125	0.075	0.05	0.07	0.016	0.086	0.01
	$\theta = 90^o$	0.175	0.15	0.125	0.05	0.16	0.09	0.1	0.08

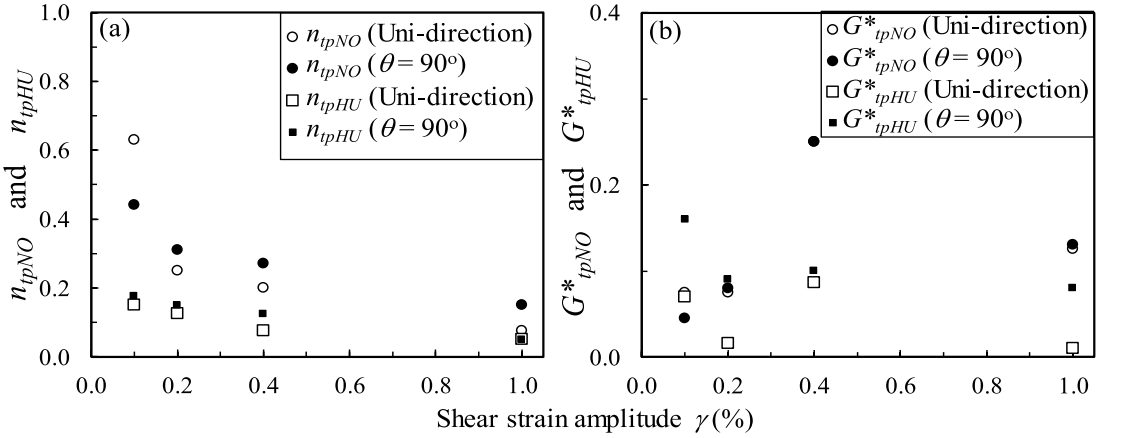

Figure 9. Changes of n_{tpNO}, n_{tpHU}, G^*_{tpNO} and G^*_{tpHU} with γ for Nam O sand and Hue clay subjected to undrained cyclic shear

3.3. Relations of u_{acc}/σ'_{vo} versus γ and G for different cyclic shear conditions*

In Fig. 10(a), obtained results of u_{acc}/σ'_{vo} are shown against γ for all specimens of Nam O sand and Hue clay used in this study. Sandy soils, especially at loose and medium density are confirmed to be liquefied easily when subjected to cyclic loading and consequently, almost results of u_{acc}/σ'_{vo} obtained for specimen at D_r = 50%±5% of Nam O sand are equal to unity (i.e. u_{acc}/σ'_{vo} = 1). Meanwhile, the pore water pressure ratio of Hue clay increases with γ and at the same n and γ, two-directional cyclic shears induce considerably higher u_{acc}/σ'_{vo} than those generated by the uni-directional one. This observation suggests the influence of the cyclic shear direction on the pore water pressure response of Hue clay, and such an effect remains for a wide range of γ (γ = 0.1%-1.0%) and a relatively large n (n = 200). As to Nam O sand, discrepancies of u_{acc}/σ'_{vo} between the uni-direction and two-direction are observed only for $\gamma \leq 0.1\%$. When $\gamma \geq 0.1\%$, nominally 50% relative density specimen of Nam O sand is liquefied quickly and therefore such effects of the cyclic shear direction become negligible.

Because the cyclic shear tests on Nam O sand were run with different number of cycles (n = 10, 50 and 150) and the differences of u_{acc}/σ'_{vo} between the uni-direction and two-direction are evident on Hue clay, then relations between u_{acc}/σ'_{vo} and γ show several scattering as seen in Fig. 10(a). Meanwhile, by using G^* as shown in Fig. 10(b), the tendencies of u_{acc}/σ'_{vo} become more unique and based on which, fitting dashed- and solid-lines can be referred to a prediction of the pore water pressure accumulation in Nam O sand and Hue clay subjected to undrained uni-directional and two-directional cyclic shears.

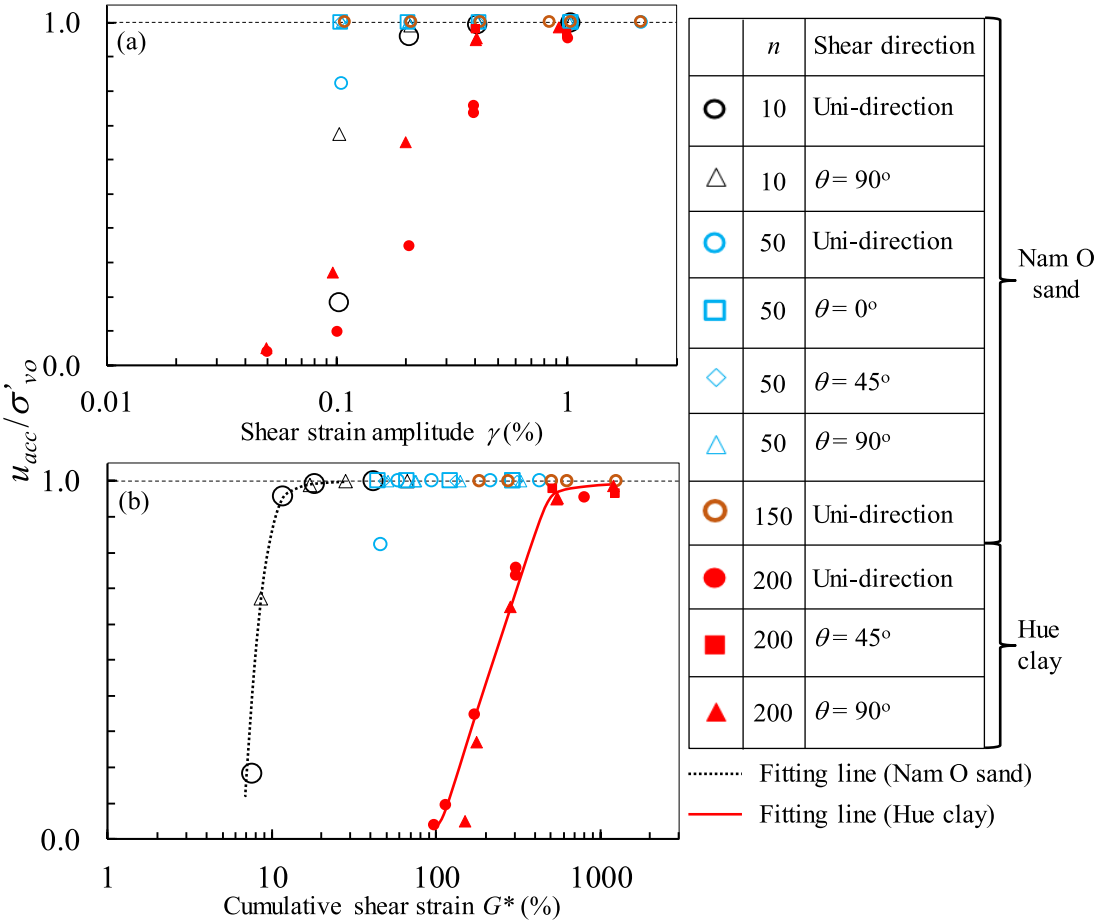

Figure 10. Changes of u_{acc}/σ'_{vo} versus γ and G^* for Nam O sand and Hue clay subjected to undrained cyclic shear with various conditions

4. Conclusions

The main conclusions are as follows:

(1) The length of the strain path induced by cyclic simple shearing can be expressed by $G^* = 4 \times \gamma \times n$ and $G^* = 6.3084 \times \gamma \times n$ for the uni-directional and two-directional cyclic shear, respectively.

(2) Under the same cyclic shear conditions, the pore water pressure accumulation in Nam O sand is quicker than that in Hue clay and consequently, soft specimens of Hue clay at relatively low plasticity shows a higher cyclic shear resistance than the nominally 50% relative density specimens of Nam O sand.

(3) Nam O sand is liquefied just after several cycles of the undrained cyclic shearing application when $\gamma \geq 0.4\%$ meanwhile, the phenomenon is not reached in Hue clay even for the case of two-directional cyclic shear with $\gamma = 1.0\%$ and $n = 200$.

(4) n_{tpNO} and n_{tpHU} generally decrease with γ meanwhile, a relation of $G^*_{tpNO} = G^*_{tpHU} = 0.1\%$ can be referred to as the threshold cumulative shear strain for the pore water pressure generation in Nam O sand and Hue clay subjected to undrained uni-directional and two-directional cyclic shears.

(5) By using G^* instead of γ, tendencies of the pore water pressure accumulation on each soil become more unique. It is suggested that G^* shows more advantageous when

evaluating the cyclic shear-induced pore water pressure responses of the soils.

Acknowledgements

This research is funded by Vietnam National Foundation for Science and Technology Development (NAFOSTED) under Grant Number 105.08-2018.01 and by Hue University under the Core Research Program, Grant No. NCM.DHH.2018.03. The experimental works were supported by students who graduated from Yamaguchi University. The authors would like to express their gratitude to them.

References

Bhattacharya S., Hyodo M., Goda K., Tazoh T., Taylor C.A., 2011. Liquefaction of soil in the Tokyo Bay area from the 2011 Tohoku (Japan) earthquake. Soil Dynamics and Earthquake Engineering, 31(11), 1618-1628.

Fukutake K., Matsuoka H.A., 1989. Unified law for dilatancy under multi-directional simple shearing. Journal of JSCE Division C, JSCE, 412(III-1), 143-151 (in Japanese).

Gratchev I.B., Sassa K., Osipov V.I., Sokolov V.N., 2006. The liquefaction of clayey soils under cyclic loading. Engineering Geology Journal, 86(1), 70-84.

Matasovic N., Vucetic M., 1992. A pore pressure model for cyclic straining of clay. Soils and Foundations, 32(3), 156-173.

Matasovic N., Vucetic M., 1995. Generalized cyclic degradation pore pressure generation model for clays. Journal of Geotechnical Engineering, ASCE, 121(1), 33-42.

Matsuda H., 1997. Estimation of post-earthquake settlement-time relations of clay layers. Journal of JSCE Division C, JSCE, 568(III-39), 41-48 (in Japanese).

Matsuda H., Nhan T.T., Ishikura R., 2013. Prediction of excess pore water pressure and post-cyclic settlement on soft clay induced by uni-directional and multi-directional cyclic shears as a function of strain path parameters. Soil Dynamics and Earthquake Engineering, 49, 75-88.

Mendoza M.J., Auvinet G., 1988. The Mexico Earthquake of September 19, 1985-Behaviour of building foundations in Mexico City. Earthquake Spectra, 4(4), 835-852.

Ministry of Science and Technology (MOST), 2012. Design of structures for earthquake resistance - Part 1: General rules, seismic actions and rules for buildings; Part 2: Foundations, retaining structures and geotechnical aspects. TCVN-9386: 2012, Vietnam, 230p.

Nhan T.T., 2013. Study on excess pore water pressure and post-cyclic settlement of normally consolidated clay subjected to uniform and irregular cyclic shears. Doctoral dissertation, Yamaguchi University, Japan, 131p.

Nhan T.T., 2019. Liquefaction resistance and post-cyclic settlement of Nam O sand subjected to uni-directional and multi-directional cyclic shears. Lecture Notes in Civil Engineering, 18, 102-107.

Nhan T.T., Matsuda H., 2020. Pore water pressure accumulation and settlement of clays with a wide range of Atterberg's limits subjected to multi-directional cyclic shear. Vietnam Journal of Earth Science, 42(1), 2615-9783.

Nhan T.T., Matsuda H., Sato H., Thien D.Q., Tien P.V., Nhan N.T.T., Forthcoming, 2022. Pore water pressure and settlement of clays under cyclic shear: concerning the effect of soil plasticity and cyclic shear direcion. Journal of Geotechnical and Geoenvironmental Engineering.
Doi: 10.1061/(ASCE)GT.1943-5606.0002734.

Ohara S., Yamamoto T., Ikuta H., 1981. Shear strength of saturated clay pre-subjected to cyclic shear. Proceedings of the Japan Society of Civil Engineers, 315, 75-82 (in Japanese).

Sasaki Y., Taniguchi E., Matsuo O., Tateyama S., 1980. Damage of soil structures by earthquakes. Public Works Research Institute, Technical Note of PWRI No. 1576 (in Japanese).

Seed H.B., 1979. Soil liquefaction and cyclic mobility evaluation for level ground during earthquakes. Journal of Geotechnical Engineering, ASCE, 105, GT2, 201-255.

Suzuki, T., 1984. Settlement of saturated clays under dynamic stress history. Journal of the Japan Society of Engineering Geology, 25(3), 21-31 (in Japanese).

Talesnick M., Frydman S., 1992. Irrecoverable and overall strains in cyclic shear of soft clay. Soils and Foundations, 32(3), 47-60.

Tin T.N., 2019. Assessment of the liquefaction resistance of sandy soils in Quang Tri coastal plain based on standard penetration test and cyclic shear test. Master thesis, Hue University of Sciences, Vietnam, 69p.

Tokimatsu K., Katsumata K., 2012. Liquefaction-induced damage to buildings in Urayasu city during the 2011 Tohoku Pacific earthquake. International Symposium on Engineering Lessons Learned from the 2011 Great East Japan Earthquake, 665-674.

Tokue T., 1976. Characteristics and mechanism of vibratory densification of sand and role of acceleration. Soils and Foundations, 16(3), 1-18.

Vy T.T.B., 2007. Establishment of the engineering geological map at large scale for Hue city and surrounding areas. Master thesis, Hue University of Sciences, Vietnam, 78p.

Yasuhara K., Andersen K.H., 1991. Recompression of normally consolidated clay after cyclic loading. Soils and Foundations, 31(1), 83-94.

Yasuhara K., Hirao K., Hyde A.F.L., 1992. Effects of cyclic loading on undrained strength and compressibility of clay. Soils and Foundations, 32(1), 100-116.

Yasuhara K., Murakami S., Toyota N., Hyde A.F.L., 2001. Settlements in fine-grained soils under cyclic loading. Soils and Foundations, 41(6), 25-36.

Zeevaert L., 1983. Foundation engineering for difficult subsoil conditions. Van Nostrand Co. Ltd (2nd Edition), New York, USA.